JOURNAL OF AGRICULTURAL AND FOOD CHEMISTRY
ARTICLE

J. Agric. Food Chem. 2011, 59, 145–151 145
DOI:10.1021/jf1033224

Pharmacokinetic Study of Nobiletin and Tangeretin in Rat Serum by High-Performance Liquid Chromatography−Electrospray Ionization−Mass Spectrometry

JOHN A. MANTHEY,*,† THAIS B. CESAR,§ ERIN JACKSON,# AND SUSANNE MERTENS-TALCOTT#

†Citrus and Subtropical Products Research Laboratory, Agricultural Research Service, U.S. Department of Agriculture, 600 Avenue S, N.W., Winter Haven, Florida 33881, United States, §Department of Nutrition, São Paulo State University, São Paulo, Brazil, and #Department of Nutrition and Food Science, Institute for Obesity Research and Program Evaluation, Texas A&M University, College Station, Texas 77845, United States

Nobiletin (NOB) and tangeretin (TAN), two of the main polymethoxylated flavones (PMFs) in citrus, influence a number of key biological pathways in mammalian cells. Although the impacts of NOB and TAN on glucose homeostasis and cholesterol regulation have been investigated in human clinical trials, much information is still lacking about the metabolism and oral bioavailability of these compounds in animals. In this study, NOB and TAN were administered to rats by gavage and intraperitoneal (ip) injection, and the blood serum concentrations of these compounds and their main metabolites were monitored by high-performance liquid chromatography−electrospray ionization−mass spectrometry (HPLC-ESI-MS). In addition to the administered compounds, two metabolites of TAN and eight metabolites of NOB were detected and measured over 24 h. With identical oral doses, nearly 10-fold higher absorption of NOB occurred compared to TAN. For both compounds, maximum levels of glucuronidated metabolites occurred in the blood serum at later time points (∼5−8 h) compared to the earlier T_{max} values for NOB and TAN. In most cases the glucuronides occurred at substantially higher concentrations than the aglycone metabolites. Low levels of NOB and TAN and their metabolites were detectable in rat blood serum even at 24 h after treatment.

KEYWORDS: Nobiletin; tangeretin; demethylnobiletin; demethyltangeretin; pharmacokinetics; glucuronides; metabolites; bioavailability; flavonoids; Rutaceae

INTRODUCTION

Nobiletin (NOB) and tangeretin (TAN) are two of the main polymethoxylated flavones (PMFs) in *Citrus reticulata* (tangerine), *Citrus sinensis* (sweet orange), *Citrus paradisi* (grapefruit), and *Citrus aurantium* L. (sour orange) (*1*, *2*). In tangerines NOB and TAN typically constitute the majority of the total PMFs (*3*), whereas in grapefruit and sweet orange a number of other PMFs also comprise significant portions of the total PMF content (*2*, *4*). These compounds have been shown to influence a variety of biochemical events in mammalian cells, particularly in pathways associated with in vitro cancer cell proliferation, lipid biosynthesis, and inflammation (*5*). The biological properties of both NOB and TAN have been studied in small-animal and human clinical trials and have been shown to significantly decrease serum triglycerides, total cholesterol, and LDL- and VLDL-cholesterol levels (*6*, *7*). Significant impacts were also observed in beneficially influencing glucose tolerance (*8*). Yet, further characterizations of the metabolism and the biochemical factors influencing these compounds' pharmacokinetics are critically needed, especially because oral bioavailability appears to be a significant limiting factor to the efficacy of these and other citrus PMFs (*9*).

Metabolites of PMFs have been previously studied in cell culture (*10*, *11*), animal tissues (*12*−*15*), and in vivo (*6*, *9*, *16*−*18*), yet the emphasis of these studies has been nearly exclusively on the flavone portions of these compounds, whereas much less has been reported about the intact glucuronidated metabolites, although profiles of the glucuronides of NOB and TAN metabolites in hamsters and of 3,5,6,7,8,3′,4′-heptamethoxyflavone in rats have been preliminarily described (*6*, *9*).

Studies of the metabolism of the PMFs have also provided evidence of the roles of oxidative demethylation by a number of different cytochrome P450 isozymes (*12*, *19*), and structures of the aglycone metabolites of TAN (*14*, *16*) and NOB (*17*, *20*) are consistent with such P450-catalyzed modifications. Furthermore, recent reports of the biological actions of these aglycone metabolites suggest that these compounds may be important to the overall expression of biological actions of NOB and TAN in animals (*21*−*24*). To help achieve a fuller understanding of the potential scope of biological actions of TAN and NOB in animals,

*Author to whom correspondence should be addressed [phone (863) 293-4133; fax (863) 299-8678; e-mail John.Manthey@ars.usda.gov].

Published on Web 12/06/2010

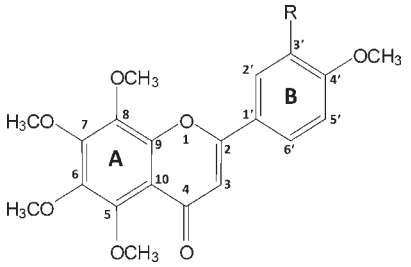

Figure 1. Structures of NOB (R = OCH_3) and TAN (R = H). Heterocyclic ring atoms are labeled for interpretation of ^1H and ^{13}C NMR data.

our study characterizes the time courses of NOB and TAN in the serum of rats administered these compounds via different modes and formulations. Particular attention is also given to the time courses of the serum levels of the metabolites of NOB and TAN, including their glucuronidated forms.

MATERIALS AND METHODS

Chemicals and Reagents. NOB and TAN (**Figure 1**) were isolated from nonvolatile residues of vacuum-distilled orange oil produced at a local chemical company. Oil residue (25 g of 30% PMF content) was stirred in 250 mL of methanol at room temperature for 2 h. The mixture was allowed to settle, and the PMF-containing methanol solution was decanted. The oil residue was re-extracted in an identical manner, and the two decanted PMF-containing methanol solutions were combined, evaporated, and dried onto silica gel (200 g) to form a free-flowing powder for chromatographic separations. Purified NOB and TAN were obtained according to methods previously reported (*25*, *26*). Hesperetin (3′,5,7-trihydroxy-4′-methoxyflavanone) was obtained commercially (Sigma, St. Louis, MO).

Animal Experimental Protocol for Metabolite Isolation. Metabolites of TAN and NOB were obtained from urine of male Winstar (100−150 g) rats fed diets of rat chow containing 1% (w/w) of a NOB/TAN mixture (1:3 w/w) for 4 weeks. Animals were housed in a room maintained at a constant temperature range of 24−26 °C with a 12 h light−dark cycle and had free access to food and water. Urine from each animal was collected every week on three consecutive days (days 5, 6, and 7 of each week) and pooled and lyophilized. The animal protocol implemented in this study was in accordance with the Canadian Council of Animal Care guidelines and was approved by the University of Western Ontario Council on Animal Care.

Animal Experimental Protocol for Pharmacokinetics Study. All animals were housed and all experiments performed according to the policies and guidelines of the Institutional Animal Care and Use Committee (IACUC) of Texas A&M University, College Station, TX. Male Sprague−Dawley rats weighing 350−400 g were used in this study. The animals were not fasted and had free access to food and water during the experiment except for the first 2 h after drug administration. Each of the pharmacokinetic studies was conducted with 10 animals.

Oral doses of NOB and TAN (50 mg kg^{-1} of body weight) were prepared in ultrapure corn oil (Sigma-Aldrich, St. Louis, MO) by mixing the powdered compound with warm oil at 70 °C. Corn oil was used as the vehicle control. All preparations were cooled to room temperature prior to oral administration by gavage. The stock solutions of compounds in corn oil were 10 mg mL^{-1} of corn oil. The administered volume of corn oil with compounds was 5 mL kg^{-1}. After administration of TAN by gavage, blood samples (500 μL) were collected from the sublingual vein at 1, 2, 3, 4, 6, 8, and 24 h, as previously reported (*27*). For TAN administration by intraperitoneal (ip) injection, TAN was initially dissolved in corn oil and administered at the same concentrations and doses as for the oral administration. Blood collections also were performed at 0.5, 1, 2, 4, 8, 12, and 24 h in the same manner as for the oral administrations. The variability of the weight of each animal between both periods was not higher than 20%.

Following administration by gavage of NOB dissolved in corn oil, blood samples (500 μL) were collected from the sublingual vein at 0.5, 4, 8, and 12 h. Following administration by gavage of NOB suspended in corn oil, blood samples were collected from the sublingual vein at 0, 1, 2, and 3 h. Prior to blood collections, the rats were anesthetized with isofluorane, and after the sampling procedures, 1.0 mL of isotonic saline was replaced via ip injection to maintain blood volume in the animals. Blood samples were centrifuged at 2800*g* for 15 min at room temperature. Serum was collected and stored at −80 °C prior to analysis.

NOB and TAN Metabolite Isolations. Freeze-dried urine samples from the NOB/TAN-fed male Winstar rats were combined with distilled water (200 mL) and extracted three times with equal volumes of ethyl acetate. The less polar aglycone metabolites of TAN and NOB were extracted into the ethyl acetate, whereas the polar conjugated metabolites largely remained in the aqueous layer. The aqueous layer was partially evaporated to remove any remaining ethyl acetate and subsequently passed through a series of five C18 Sep Pacs (360 mg of resin/cartridge) (Waters, Milford, MA) preconditioned with methanol and water washes. The metabolites were eluted from the C18 Sep Pacs with 80% methanol. The recovered metabolites were dried under vacuum with an SC-110 Speedvac centrifugal evaporator (Savant, Holbrook, NY).

A Fast Centrifugal Partition Chromatography (FCPC) (Kromaton, Angers, France) unit equipped with an A200 rotor was used for initial fractionations of the complex profiles of metabolites in the ethyl acetate and aqueous phases. The adjoining HPLC system consisted of a Waters Delta 600 pump, a Waters 600 controller, a sample injector (Rheodyne, Cotati, CA) with a 10 mL loop, and a Waters 996 photodiode array detector. Data were analyzed with MassLynx ver. 3.6. The conjugated metabolites were fractionated using a biphasic solvent system composed of chloroform/methanol/water (4:5:2.5, v/v/v). Equal volumes (10 mL) of each phase were combined and added to 45 mg of dried metabolite mixture. The stationary and mobile phases were the organic and aqueous phases, respectively, where the rotor speed was 1000 rpm. The injection volume was 10 mL, and the flow rate was 5 mL min^{-1} with 1 min fractions, where every fifth fraction was analyzed by HPLC. Peaks were monitored at 330 nm. Fractionation of the less polar aglycones was achieved using the biphasic system hexane/ethyl acetate/methanol/water (1:1.2:1:1, v/v/v/v) with the aqueous phase as the mobile phase. Identical chromatographic conditions were used as described above.

Further purifications of the FCPC-fractionated metabolites were achieved by preparative-scale TLC and HPLC. Tapered TLC plates (Analtech, Newark, DE) were used primarily to isolate the aglycone metabolites. The two main TLC solvent systems included (1) hexane/*n*-butanol/formic acid (85:15:1, v/v/v) and benzene/acetone (4:1, v/v). Final isolations, particularly of glucuronidated metabolites, were achieved using Varian ProStar model 210 solvent delivery modules (Varian, Walnut Creek, CA) in conjunction with a ProStar UV−vis photodiode array detector equipped with a preparative flow cell. Compound separations were achieved using a Waters Atlantis C18 5 μm (19 × 100 mm i.d.) column. Elution conditions included gradients of aqueous 0.5% formic acid/acetonitrile, initially composed of 75:25 (v/v), and increased in acetonitrile content with linear gradients to 75:25, 65:35, 60:40, and 55:45 and then decreased to 50:50, 75:25, and 75:25 (v/v) at 6, 15, 30, 40, 45, 50, and 55 min, respectively, at a flow rate of 5.0 mL min^{-1}. Eluted compounds were monitored at 330 and 360 nm and scanned between 240 and 500 nm.

Quantitative HPLC-MS Analysis for Serum Metabolites. Thawed serum samples (200 μL) were combined with 600 μL of methanol and centrifuged at 20000*g* for 5 min at room temperature. Hesperetin, as an internal standard, was added to the clarified serum extract to a final concentration of 0.65 μg mL^{-1}. The metabolites in the rat sera were analyzed by HPLC-MS, using a Waters 2695 Alliance HPLC (Waters) connected in parallel with a Waters 996 photodiode array (PDA) detector and a Waters/Micromass ZQ single-quadrupole mass spectrometer equipped with an electrospray ionization source. Postcolumn split to the PDA and mass ZQ detector was 10:1. Compound separations were achieved with a Waters XBridge C8 column (4.6 × 150 mm i.d.). Elution conditions included gradients of aqueous 0.5% formic acid/acetonitrile, initially composed of 90:10 (v/v), and increased in acetonitrile content with linear gradient to 80:20, 75:25, 60:40, 30:70, 30:70 and then decreased to 90:10 (v/v) at 10, 15, 23, 40, 45, and 53, min, respectively, at a flow rate of 0.75 mL min^{-1}. Data handling was done with MassLynx software ver. 4.1 (Micromass, Division of Waters Corp., Beverly, MA). MS parameters were as follows: ionization mode, ES^+; capillary voltage, 3.0 kV; extractor voltage, 5 V; source temperature, 100 °C; desolvation temperature, 225 °C; desolvation N_2 flow, 465 L h^{-1}; cone N_2 flow, 0 L h^{-1}; cone voltage, 20 V.

Quantifications of the NOB and TAN metabolites were made using integrated mass-extracted total ion chromatogram (TIC) peak areas (PA) obtained in the single ion response (SIR) mode at the m/z $[M+H]^+$ for each compound. To normalize the mass spectrometer response during sequential runs, hesperetin was additionally measured at m/z 303 as an internal standard. NOB and TAN levels in the serum samples were calculated using SIR PA μg^{-1} response factors measured for authentic NOB and TAN standards. Levels of the metabolites N1−N8 and T1 and T2 were calculated using response factors similarly measured for these compounds.

RESULTS

Metabolite Isolation and Analysis. Complex profiles of glucuronidated and aglycone metabolites were detected in the urine of NOB/TAN-fed Winstar rats (**Figure 2**), and of these, eight were isolated that coeluted with metabolites also detected in the blood serum samples of the male Sprague−Dawley rats used in the pharmacokinetic study. These compounds were used as standards for quantification purposes and were also preliminarily analyzed by ESI-MS and FTIR spectroscopy (**Table 1**). Among these compounds, four glucuronic acid conjugates were detected, including metabolites N1, N2, N4, and T1. The ESI-MS of each of these compounds exhibited neutral losses of 176 amu, which were suggestive of the loss of glucuronic acid substituents (*6*, *9*). ^{13}C NMR spectra of N1 and N2 exhibited resonances consistent with glucuronic acid conjugation (data not shown). The detection of carboxyl carbonyl vibrations near 1736 cm^{-1} in the FTIR spectra of each of these compounds also supported the presence of glucuronic acid substituents in these compounds. The fragment ions at m/z 389 of N1 and N2 suggest mono-demethylNOB structures for these metabolites, whereas the m/z 375 fragment ion suggests a didemethylNOB structure for N4. Compounds N1, N2, and N4 exhibited exact peak overlaps with the 20.6, 20.0, and 18.9 min metabolites, respectively, detected in blood sera of rats administered NOB.

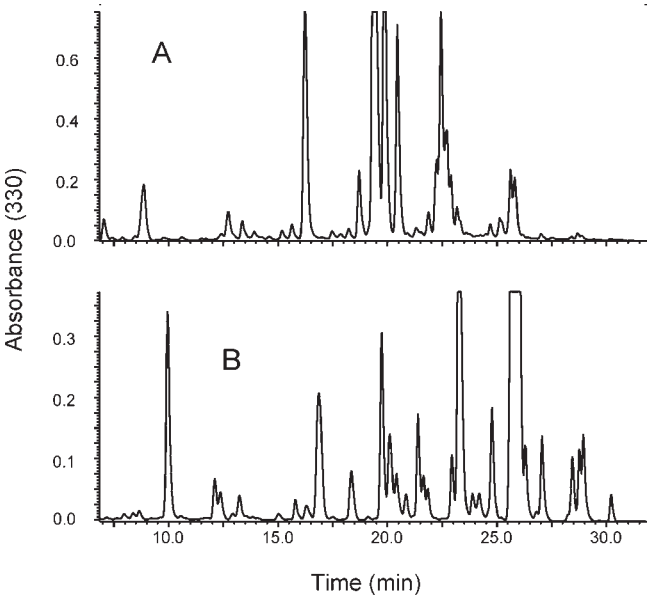

Figure 2. HPLC of NOB and TAN metabolites in urine of male Winstar rats fed diets of rat chow containing 1% NOB/TAN (1:3 w/w): (**A**) aqueous phase enriched in metabolite glucuronides; (**B**) ethyl acetate phase enriched in metabolite aglycones. Nearly all peaks exhibit UV spectra of flavones, specifically similar to either NOB or TAN.

Metabolite T1 isolated from urine of rats administered TAN exhibited a $[M+H]^+$ ion at m/z 535 and a major fragment ion of m/z 359 (**Table 1**) and showed exact peak overlap with a serum m/z 535 metabolite eluting at 19.0 min (data not shown). The m/z 359 fragment ion is suggestive of a mono-demethylTAN metabolite. As described above, the neutral loss of 176 amu represented by the mass differences between the m/z 535 and 359 ions and an observed carboxyl carbonyl (C═O) stretch at 1736 cm^{-1} are consistent with the presence of a glucuronic acid residue. An intense out-of-plane C−H bending mode at 837 cm^{-1} provides evidence of para substitution on the flavone B-ring. The ^1H and ^{13}C NMR of T1 exhibit resonances attributable to four methoxyls on the flavone A-ring (**Table 2**), thus further supporting the FTIR data indicating demethylation of T1 at the B-ring 4′-position.

In addition to the glucuronides, four aglycone metabolites of TAN and NOB were also isolated. Metabolite T2 exhibited a $[M+H]^+$ of m/z 359, suggestive of a mono-demethylTAN structure. The ^{13}C and ^1H NMR spectra of T2 were consistent with 4′-hydroxy-5,6,7,8-tretramethoxyflavone (**Table 2**) and matched that published by Nielsen et al. (*16*). T2 exhibited exact peak overlap and ESI-MS properties with the 25.3 min metabolite detected in the sera of rats administered TAN. As with T1, an intense out-of-plane C−H bending mode at 837 cm^{-1} provides indication of para substitution of the flavone B-ring of T2 (**Table 1**). The ^{13}C NMR of T1 exhibits resonances attributable to a carboxyl (170.05 ppm) and to four CH−OH carbons (**Table 2**) of a glucuronic acid substituent. Metabolites N5, N7, and N8 exhibited $[M+H]^+$ ions of m/z 389 suggestive of mono-demethylNOB structures. These metabolites exhibited exact ESI-MS and peak overlaps with the 23.3, 24.8, and 25.4 min metabolites, respectively, in the sera of rats administered NOB.

Metabolite Detection. Calibration curves for the detection of the $[M+H]^+$ ions of NOB (m/z 403) and TAN (m/z 373) using the ESI-MS SIR mode were linear at very low concentrations (< 1 ng) (**Figure 3A**). Gradually decreased ESI-MS SIR responses occurred at higher concentrations, with good curve fitting occurring for NOB from as high as 0.035 μg to < 19 pg and for TAN from as high as 0.05 μg to < 40 pg. The lower limits of detection (S/N > 10) using the SIR mode were ∼2 and 4 pg for NOB and TAN, respectively. In contrast, for measurements taken in the scanning mode (100−900 amu, 1 s scan) the lower detection limits of NOB and TAN were 174 and 344 pg, respectively. In the scan mode, linear responses for the detection of NOB and TAN occurred up to ∼0.02 μg.

Table 1. Spectral Properties of TAN and NOB Metabolites

			FTIR (cm^{-1})				
compd	elution time (min)	ESI-MS (amu) (neutral loss)	carboxyl υ (C═O)	flavone υ (C═O)	phenyl ring υ (C═C)	υ (C—O)	υ (C—H)
N1	20.6	565/389 (176)	1732	1633	1515	1107, 1080, 1043, 1013	
N2	20.0	565/389 (176)	1729	1629	1515	1108, 1077, 1039, 1017	
N4	18.9	551/375 (176)	1729	1629	1506	1108, 1073, 1038, 1018	
N5	23.3	389		1629/1588	1515	1144, 1113, 1070, 1039	
N7	24.8	389		1635/1597	1515	1146, 1102, 1071, 1043	
N8	25.4	389		1629/1590	1515	1134, 1109, 1076, 1038	
T1	19.0	535/359 (176)	1736	1624/1594	1510	1096, 1074, 1038, 1008	837
T2	25.3	359		1622/1575	1512	1111, 1076, 1037, 1011	837

Beyond this amount, signal saturation occurred. Similar mass spectral detection response analyses were made for T2 and N8 (**Figure 3B**) and for the remaining metabolite aglycones (data not shown). For the flavone glucuronides, N1 and N2, linear responses with the ESI-MS SIR detection mode were observed. Minimum levels of detection by ESI-MS SIR for both of these compounds, for which S/N > 10, occurred at approximately 20 pg.

Pharmacokinetics. The administration of TAN (50 mg kg^{-1} of body weight) dissolved in corn oil to rats by either gavage or ip injection resulted in the detection by HPLC-MS of TAN and two main metabolites, T1 and T2, in rat blood serum. Following ip injection, the average maximal concentration of TAN in the blood serum occurred at 4.5 μg mL^{-1} at 0.5 h. Blood serum levels of TAN then decreased rapidly over the first 5 h to approximately 1.1 μg mL^{-1} (**Figure 4**). Subsequent gradual decreases to 0.65 μg mL^{-1} occurred 12 h after administration, with detectable levels of TAN (~0.3 μg mL^{-1}) remaining in the blood serum samples 24 h after administration. The average maximum level (1.6 μg mL^{-1}) of the aglycone metabolite, T2, occurred at 0.5 h after ip injection and decreased in a manner similar to that of TAN. The time course for the glucuronic acid conjugate, T1, showed the highest serum concentration (1.7 μg mL^{-1}) at 2 h and decreased more gradually than TAN and T2. Detectable levels of both T1 and T2 remained in the rat blood sera even at 24 h after administration.

Administration of TAN by gavage (50 mg kg^{-1} of body weight) produced much lower initial TAN serum content (0.49 μg mL^{-1} at 1 h) compared to ip injection and gradually decreased in concentration to 0.16 μg mL^{-1} at 8 h (**Figure 5**). The aglycone metabolite, T2, exhibited highest concentrations between 4 and 6 h (0.38 μg mL^{-1}) and then gradually decreased by 24 h. The combined average maximum concentration at 2 h for TAN and T2 averaged < 0.8 μg mL^{-1}. The glucuronic acid conjugate, T1, similarly exhibited a broad T_{max} range between 3 and 6 h with an average highest concentration of 1.45 μg mL^{-1}. Hence, T1 represents the main chemical species in the rat blood serum following oral administration of TAN.

Table 2. ^{1}H NMR and ^{13}C NMR of TAN Metabolites

	^{1}H chemical shifts (ppm) and multiplicity[a]			^{13}C chemical shifts[b] (ppm)	
proton	T1	T2	carbon	T1	T2
phenyl-OH		10.46	C-4	175.77	175.66
H-3	6.79	6.67	C-carboxyl	170.05	
H-2′	8.01 d	7.89 d	C-4′	160.11	161.05
H-3′	7.22 d	6.94 d	C-2	159.53	160.81
H-5′	7.22 d	6.94 d	C-7	150.96	150.80
H-6′	8.01 d	7.89 d	C-5	147.49	147.45
OCH_3	4.03	4.02	C-9	147.13	147.05
	3.98	3.96	C-6	143.58	143.47
	3.85	3.84	C-8	137.74	137.70
	3.79	3.78		132.83	
				129.22	
gluc H−COH		5.72 br, 1H		128.54	
gluc H−COH		5.27 br, 1H	C-6′,2′	127.67	127.84
gluc H−COH		5.22 d, 1H	C-1′	124.47	121.13
			C-3′,5′	116.56	116.05
			C-10	114.30	114.26
			C-3	106.43	105.31
				99.39	
			C−OH glucuronic acid	75.72	
			C−OH glucuronic acid	75.37	
			C−OH glucuronic acid	72.85	
			C−OH glucuronic acid	71.28	
			A-ring methoxyl	61.88	69.75
			A-ring methoxyl	61.88	61.82
			A-ring methoxyl	61.49	61.46
			A-ring methoxyl	61.36	61.33

[a] d, doublet; br, broad. [b] Tentative assignments based on previous assignments of TAN (*33*).

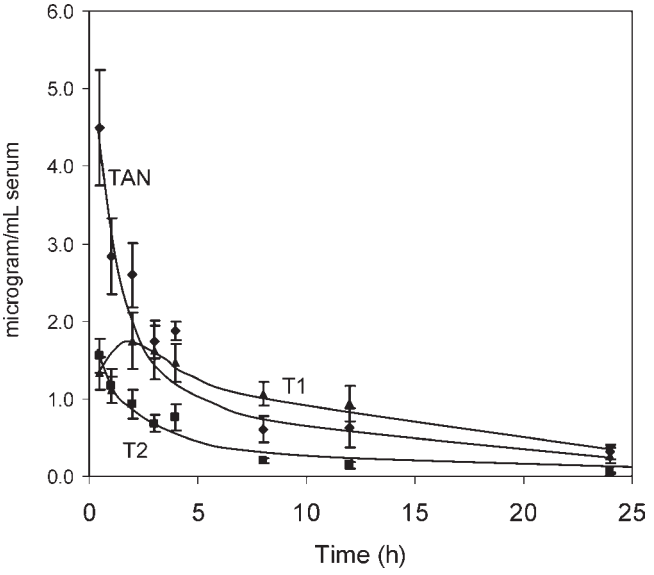

Figure 4. Pharmacokinetics of TAN (◆) and metabolites T1 (▲) and T2 (■) in rat serum following ip injection at a dose of 50 mg kg^{-1} of body weight.

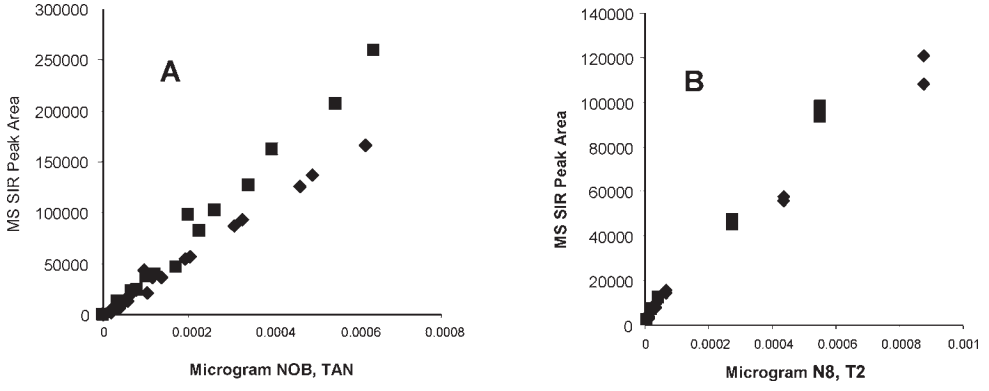

Figure 3. Calibration curves (SIR $PA_{(mwt)}$ vs μg) for the detection of the $[M + H]^+$ ions of NOB (*m/z* 403) (◆) and TAN (*m/z* 373) (■) (**A**) and N8 (*m/z* 389) (■) and T2 (*m/z* 359) (◆) (**B**).

The administration of NOB, dissolved in corn oil, by gavage produced a peak NOB serum level of 9.03 μg mL^{-1} as early as 0.5 h (**Figure 6**). There was a gradual decrease in blood serum levels, which remained above 2 μg mL^{-1} even 12 h after administration. A sharply contrasting time course of NOB absorption was observed when NOB was administered as a solid precipitate suspended in corn oil (**Figure 6**). Following gavage administration of the suspension the blood serum, NOB levels increased gradually to 3.21 μg mL^{-1} at 2 h and then showed a substantial decline at 3 h.

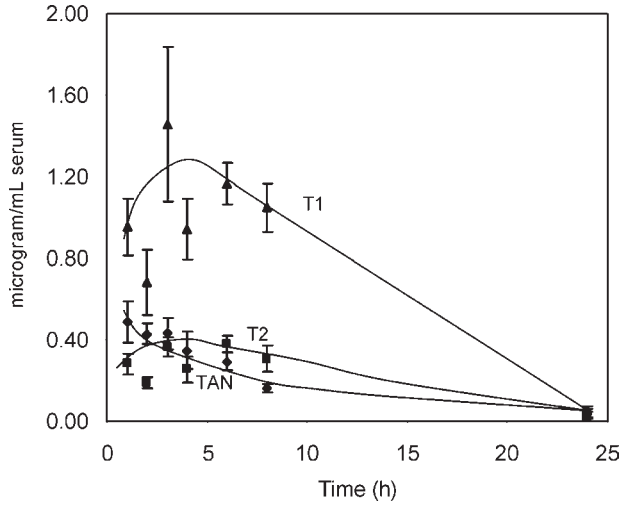

Figure 5. Pharmacokinetics of TAN (◆) and metabolites T1 (▲) and T2 (■) in rat serum following administration by gavage at a dose of 50 mg kg^{-1} of body weight.

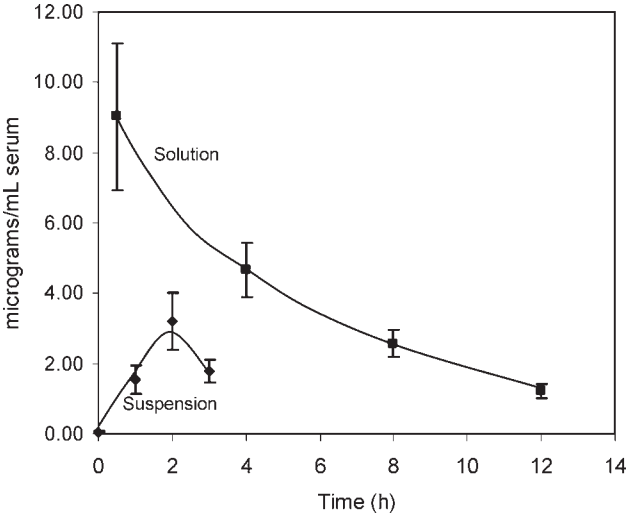

Figure 6. Pharmacokinetics of NOB administered at a dose of 50 mg kg^{-1} of body weight to rats by gavage as a dissolved solution or as a suspension in corn oil.

Eight metabolites of NOB (N1−N8) were detected in the blood serum of rats administered NOB dissolved in corn oil by gavage (50 mg kg^{-1} of body weight) (**Table 3**). Structural data of metabolites N1, N2, N4, N5, N7, and N8 have been previously presented in **Table 1**. Metabolites N3 and N6 exhibited ESI-MS similar to those of N1 and N2 and N5, N7, and N8, respectively, and hence are a mono-demethylNOB glucuronide and a mono-demethylNOB aglycone, respectively. Concentrations of these metabolites were measured at 0.5, 4, 8, and 12 h, and the measurements showed maximal concentrations of these compounds at 8 h. None of the aglycone metabolites, N5−N8, exceeded 0.5 μg mL^{-1} in the rat blood serum, whereas the glucuronidated metabolites, N1−N4 exhibited average maximal concentrations of 0.83, 3.28, 0.56, and 0.71 μg mL^{-1}, respectively, at 8 h. At this 8 h time point, NOB, the total NOB aglycones, and the total NOB glucuronide metabolites occurred at 2.7, 0.50, and 5.4 μg mL^{-1}, respectively.

DISCUSSION

TAN and NOB, along with the other citrus peel PMFs, exhibit distinctive chemical and physical properties relative to a majority of other plant flavonoids, and these properties likely play important roles in influencing the metabolism and pharmacokinetics of these compounds in animals. Evidence of these influences is observed in our current study by the trace levels of detection achievable by ESI-MS of TAN, NOB, and their demethylated metabolites. The metabolic pathways of NOB and TAN (*12*, *19*) and the prolonged presence of these administered compounds in the sera of dosed animals, as shown in **Figures 4**−**6**, are further evidence of the influences of the extensive methoxylation of these molecules. Using the ESI-MS SIR detection mode, NOB and TAN were detectable at levels as low as 2 and 4 pg, respectively, and similarly for the aglycone metabolites, T2 and N8 (**Figure 3**). In contrast, the lowest detectable levels for the glucuronidated metabolites (N1, N2, N4, and T1) were much higher, a reflection of the higher polarities of these compounds due to their glucuronic acid substituents.

Analysis by ESI-MS also provided important structural information about the metabolites of NOB and TAN, including the glucuronic acid conjugation in the higher molecular weight

Table 3. Concentrations of NOB Metabolites in Rat Serum

	glucuronide metabolites			
time (h)	N1: 20.3 (565 amu)	N2: 19.7 (565 amu)	N3: 17.27 (565 amu)	N4: 18.7 (551 amu)
0.5	0.053 ± 0.013	0.512 ± 0.130	0.084 ± 0.029	0.002 ± 0.000
4	0.227 ± 0.143	1.560 ± 0.735	0.174 ± 0.0847	0.028 ± 0.021
8	0.833 ± 0.392	3.281 ± 1.172	0.568 ± 0.220	0.716 ± 0.377
12	0.664 ± 0.177	0.279 ± 0.061	0.040 ± 0.006	0.147 ± 0.041
	aglycone metabolites			
time (h)	N5: 23.3 (389 amu)	N6: 23.8 (389 amu)	N7: 24.8 (389 amu)	N8: 25.8 (389 amu)
0.5	0.122 ± 0.013	0.020 ± 0.003	0.022 ± 0.006	0.020 ± 0.002
4	0.299 ± 0.134	0.006 ± 0.001	0.011 ± 0.004	0.027 ± 0.008
8	0.433 ± 0.207	0.012 ± 0.003	0.021 ± 0.007	0.034 ± 0.012
12	0.031 ± 0.007	0.002 ± 0.000	0.005 ± 0.001	0.009 ± 0.001

compounds (*6*, *9*). FTIR analysis also provided evidence supporting the glucuronidation of four of the isolated compounds listed in **Table 1** and was also useful in confirming structural details of the flavone B-rings of T1 and T2. The ^{1}H NMR data of T2 were consistent with 4′-demethylTAN (*16*), and the nearly identical ^{1}H and ^{13}C NMR of T1 and T2, along with the observation of NMR signals of T1 consistent with a glucuronic acid substituent, are also suggestive of a 4′-demethylNOB-4′-glucuronic acid structure for T1. Further work is needed to elucidate the chemical structures of the other remaining NOB and TAN metabolites listed in **Tables 1** and **3**. Many other minor metabolites of NOB and TAN illustrated in **Figure 2** also remain to be characterized.

In addition to providing preliminary information about the chemical structures of metabolites of NOB and TAN in rats, the isolated metabolites listed in **Table 1** were also used as standards for quantification purposes in the ensuing pharmacokinetic studies. These pharmacokinetic studies conducted with the male Sprague−Dawley rats showed appreciable serum levels of NOB and TAN when administered by gavage and ip injection, respectively. Results also showed that these compounds remained in the blood serum for prolonged periods up to 24 h after treatment. Specifically, administration of NOB dissolved in corn oil by gavage produced a rapid appearance of NOB (9.3 μg mL^{-1} at 0.5 h) in the rat blood sera, in which the levels of NOB remained >4 μg mL^{-1} at 4 h, >3 μg mL^{-1} at 8 h, and $\sim$2 μg mL^{-1} at 12 h. This is in contrast to a number of other previously studied hydroxylated flavonoids that are typically detected nearly exclusively in serum as glycosidated or sulfated chemical species (*28*−*31*), with only trace levels of the originally administered compounds present at later time points.

Unlike the rapid absorption of NOB administered solubilized in corn oil, gavage administration of NOB suspended as an insoluble particulate resulted in slower absorption (T_{max} 2 h) and lower maximal NOB serum levels (3.56 μg mL^{-1}). These results show that prior solubilization of NOB strongly influences the serum pharmacokinetics of NOB and, thus, may strongly influence the efficacy of NOB at given oral doses. This is likely to apply to the other citrus PMFs as well. Also of particular importance was the finding of the significantly higher NOB serum level (9.3 μg mL^{-1}) achieved when administered NOB by gavage compared to the level of TAN (0.49 μg mL^{-1}) achieved with identical dosing of TAN. This finding suggests a potentially significant difference in the bioavailabilities of NOB and TAN and, as a consequence, may also suggest possible differences in the efficacies of these two compounds when administered in animals.

Finally, the observation of the diverse metabolites of TAN and NOB in this study, and elsewhere (*6*, *9*−*16*), suggests that the total biological actions expressed by specific doses of NOB and TAN may also contain important contributions from the biological actions of these metabolites. Most recently, the major NOB metabolite, 4′-demethyl NOB, was shown to stimulate key phosphorylation pathways linked to memory processing and was further shown to be able to cross the blood−brain barrier (*32*). Earlier, Li et al. (*22*) reported that a number of NOB metabolite aglycones inhibit bacterial lipopolysaccharide-induced nitric oxide (NO) production and iNOS and cyclooxygenase (COX)-2 protein expression in RAW 264.7 macrophage and, in fact, these metabolites exhibited greater inhibitory activity than the parent compound, NOB. In a similar manner the suppression of TPA-induced expression of SR-A (oxidized LDL scavenger receptor in macrophages) and LOX-1 by the aglycone metabolites 3′-desmethyl NOB, 4′-desmethyl NOB, and 3′,4′-didesmethyl NOB was also typically more active than NOB (*21*). Analyses of the biological actions of the metabolites of TAN are lacking, but it is likely that similar biological actions might also be attributable to these compounds. Relevant to this, lower levels of serum T1 and T2 metabolites were detected after administration of TAN compared to the levels of serum NOB metabolites after identical NOB administration, but it was significant to note that TAN and T2 occurred at roughly similar levels throughout the 24 h after treatment. Thus, T2 may significantly contribute to the total activity expressed by TAN at specific doses. These findings, along with the observed presence of multiple aglycone metabolites of NOB in the rat blood serum, suggest that the study of the full scope of biological actions of the citrus PMFs needs to include pharmacokinetic analysis of the multiple, biologically active metabolites.

ACKNOWLEDGMENT

We thank Dr. Vincent Gresham, Andrea Taylor, and Ryan Byrd, all of the Comparative Medicine Program, Texas A&M University, and Veronica Cook of the Citrus and Subtropical Products Research Laboratory for their valuable contributions.

LITERATURE CITED

(1) Horowitz, R. M.; Gentili, B. Flavonoid constituents of citrus. In *Citrus Science and Technology*; Avi Publishing: Westport, CT, 1977; Vol. 1, pp 397−426.

(2) Dugo, P.; McHale, D. The oxygen heterocyclic compounds of citrus essential oils. In *Citrus. The Genus Citrus*; Dugo, G., Di Giacomo, A., Eds.; Taylor and Francis: Boca Raton, FL, 2002; pp 355−390.

(3) Gaydou, E. M.; Bianchini, J. P.; Randriamiharisoa, R. P. Orange and mandarin peel oils differentiation using polymethoxylated flavone composition. *J. Agric. Food Chem.* **1987**, *35*, 525−529.

(4) Dugo, P.; Mondello, L.; Dugo, G.; Heaton, D. M.; Bartle, K. D.; Clifford, A. A.; Myers, P. Rapid analysis of polymethoxylated flavones from citrus oils by supercritical fluid chromatography. *J. Agric. Food Chem.* **1996**, *44*, 3900−3905.

(5) Benavente-Garcia, O.; Castillo, J. Update on uses and properties of citrus flavonoids: new findings in anticancer, cardiovascular, and anti-inflammatory activity. *J. Agric. Food Chem.* **2008**, *56*, 6185−6205.

(6) Kurowska, E. M.; Manthey, J. A. Hypolipodemic effects and absorption of citrus polymethoxylated flavones in hamsters with diet-induced hypercholesterolemia. *J. Agric. Food Chem.* **2004**, *52*, 2879−2886.

(7) Roza, J. M.; Xian-Liu, Z.; Guthrie, N. Effect of citrus flavonoids and tocotrienols on serum cholesterol levels in hypercholesterolemic subjects. *Alnternative Ther.* **2007**, *13*, 44−48.

(8) Li, R. W.; Theriault, A. G.; Au, K.; Douglas, T. D.; Casachi, A.; Kurowska, E. M.; Mukherjee, R. Citrus polymethoxylated flavones improve lipid and glucose homeostasis and modulate adipocytokines in fructose-induced insulin resistant hamsters. *Life Sci.* **2006**, *79*, 365−373.

(9) Manthey, J. A.; Bendele, P. Anti-inflammatory activity of an orange peel polymethoxylated flavone, 3′,4′,3,5,6,7,8-heptamethoxyflavone, in the rat carrageenan/paw edema and mouse lipopolysaccharide-challenge assays. *J. Agric. Food Chem.* **2008**, *56*, 9399−9403.

(10) Murakami, A.; Kuwahara, S.; Takahashi, Y.; Ito, C.; Furukawa, H.; Ju-Ichi, M.; Koshimuzu, K.; Ohigashi, H. In vitro absorption and metabolism of nobiletin, a chemopreventative polymethoxyflavonoid in citrus fruits. *Biosci., Biotechnol., Biochem.* **2001**, *65*, 194−197.

(11) Buisson, D.; Quintin, J.; Lewin, G. Biotransformation of polymethoxylated flavonoids: access to their 4′-*O*-demethylated metabolites. *J. Nat. Prod.* **2007**, *70*, 1035−1038.

(12) Koga, N.; Matsuo, M.; Ohta, C.; Haraguchi, K.; Matsuoka, M.; Kato, Y.; Ishii, T.; Yano, M.; Ohta, H. Comparative study of nobiletin metabolism with liver microsomes from rats, guinea pigs and hamsters and rat cytochrome P450. *Biol. Pharm. Bull.* **2007**, *30*, 2317−2323.

(13) Breinholt, V.; Lauridsen, S. T.; Dragsted, L. O. Differential effects of dietary flavonoids on drug metabolizing and antioxidant enzymes in female rats. *Xenobiotica* **1999**, *29*, 1227−1240.

(14) Nielsen, S. E.; Brienholt, V.; Justesen, U.; Cornett, C.; Dragsted, L. O. In vitro biotransformation of flavonoids by rat liver microsomes. *Xenobiotica* **1998**, *28*, 389−401.

(15) Walle, U. K.; Walle, T. Bioavailable flavonoids: cytochrome P450-mediated metabolism of methoxyflavones. *Drug Metab. Dispos.* **2007**, *35*, 1985−1989.
(16) Nielsen, S. E.; Breinholt, V.; Cornett, C.; Dragsted, L. O. Biotransformation of the citrus flavone tangeretin in rats. Identification of metabolites with intact flavone nucleus. *Food Chem. Toxicol.* **2000**, *38*, 739−746.
(17) Yasuda, T.; Yoshimura, Y.; Yabuki, H.; Nakazawa, T.; Ohsawa, K.; Mimaki, Y.; Sashida, Y. Urinary metabolites of nobiletin orally administered to rats. *Chem. Pharm. Bull.* **2003**, *51*, 1426−1428.
(18) Murakami, A.; Koshimizu, K.; Ohigashi, H.; Kuwahara, S. Characteristic rat tissue accumulation of nobiletin, a chemopreventative polymethoxyflavonoid, in comparison with luteolin. *Biofactors* **2002**, *16*, 73−82.
(19) Breinholt, V. M.; Rasmussen, S. E.; Brosen, K.; Friedberg, T. H. In vitro metabolism of genistein and tangeretin by human and murine cytochrome P450s. *Pharmacol. Toxicol.* **2003**, *93*, 14−22.
(20) Li, S.; Wang, Z.; Sang, S.; Huang, M. T.; Ho, C. T. Identification of nobiletin metabolites in mouse urine. *Mol. Nutr. Food Res.* **2006**, *50*, 291−299.
(21) Eguchi, A.; Murakami, A.; Li, S.; Ho, C. T.; Ohigashi, H. Suppressive effects of demethylated metabolites of nobiletin on phorbol ester-induced expression of scavenger receptor genes in THP-1 human monocytic cells. *Biofactors* **2007**, *31*, 107−116.
(22) Li, S.; Sang, S.; Pan, M. H.; Lai, C. S.; Lo, C. Y.; Yang, C. S.; Ho, C. T. Anti-inflammatory property of the urinary metabolites of nobiletin in mouse. *Bioorg. Med. Chem. Lett.* **2007**, *17*, 5177−5181.
(23) Lai, C. S.; Li, S.; Chai, C. Y.; Lo, C. Y.; Dushenkov, S.; Ho, C. T.; Pan, M. H.; Wang, Y. J. Anti-inflammatory and antitumor promotional effects of a novel urinary metabolite, 3′,4′-didemethylnobiletin, derived from nobiletin. *Carcinogenesis* **2008**, *29*, 2415−2424.
(24) Xiao, H.; Yang, C. S.; Li, S.; Jin, H.; Ho, C. T.; Patel, T. Monodemethylated polymethoxyflavones from sweet orange (*Citrus sinensis*) peel inhibit growth of human lung cancer cells by apoptosis. *Mol. Nutr. Food Res.* **2009**, *53*, 398−406.
(25) Swift, L. J. TLC-spectrophotometric analysis for neutral fraction flavones in orange peel juice. *J. Agric. Food Chem.* **1967**, *15*, 99−101.
(26) Tatum, J. H.; Berry, R. E. Six new flavonoids from *Citrus*. *Phytochemistry* **1972**, *11*, 2283−2288.
(27) De Castro, W. V.; Mertens-Talcott, S.; Derendorf, H.; Butterweck, V. Effect of grapefruit juice, naringin, naringenin, and bergamottin on the intestinal carrier-mediated transport of talinolol in rats. *J. Agric. Food Chem.* **2008**, *56*, 4840−4845.
(28) Chao, P. D. L.; Hsiu, S. L.; Hou, Y. C. Flavonoids in herbs: biological fates and potential interactions with xenobiotics. *J. Food Drug Anal.* **2002**, *10*, 219−228.
(29) Manach, C.; Williamson, G.; Morand, C.; Scalbert, A.; Remesy, C. Bioavailability and bioefficacy of polyphenols in humans. I. Review of 97 bioavailability studies. *Am. J. Clin. Nutr.* **2005**, *81*, 230S−242S.
(30) Pozharitskaya, O. N.; Karlina, M. V.; Shikov, A. N.; Kosman, V. M.; Makarova, M. N.; Makarov, V. G. Determination and pharmacokinetic study of taxifolin in rabbit plasma by high-performance liquid chromatography. *Phytomedicine* **2009**, *16*, 244−251.
(31) Shia, C. S.; Tsai, S. Y.; Kuo, S. C.; Hou, Y. C.; Chao, P. D. L. Metabolism and pharmacokinetics of 3,3′,4′,7-tetrahydroxyflavone (fisetin), 5-hydroxyflavone, and 7-hydroxyflavone and antihemolysis effects of fisetin and its serum metabolites. *J. Agric. Food Chem.* **2009**, *57*, 83−89.
(32) Al Rahim, M.; Nakajima, A.; Saigusa, D.; Tetsu, N.; Maruyama, Y.; Shibuya, M.; Yamakoshi, H.; Tomioka, Y.; Iwabuchi, Y.; Ohizumi, Y.; Yamakuni, T. 4′-Demethylnobiletin, a bioactive metabolite of nobiletin enhancing PKA/ERK/CREB signaling, rescues learning impairment associated with NMDA receptor antagonism via stimulation of the ERK cascade. *Biochemistry* **2009**, *48*, 7713−7721.
(33) Iinuma, M.; Matsuura, S.; Kusuda, K. ^{13}C-Nuclear magnetic resonance (NMR) spectral studies on polysubstituted flavonoids. I. ^{13}C-NMR spectra of flavones. *Chem. Pharm. Bull.* **1980**, *28*, 708−716.

Received for review August 26, 2010. Revised manuscript received November 3, 2010. Accepted November 3, 2010. We express our gratitude to Dr. Peter Murano of the Institute for Obesity Research and Program Evaluation, Texas A&M University, College Station, TX, for funding the animal feeding trials.